Stress-strain and degradation behaviour of railway ballast under static and dynamic loading, based on large-scale triaxial testing

Comportement de dégradation et de tension dûe à la pression du ballast de chemin de fer dans des conditions de chargement statiques et dynamiques, et dans le cadre de tests triaxiaux à grande échelle

B.Indraratna & W.Salim – *University of Wollongong, Wollongong, NSW 2522, Australia*
D.Ionescu – *La Trobe University, Bendigo, VIC 3552, Australia*
D.Christie – *Rail Services Australia, Sydenham, NSW 2044, Australia*

ABSTRACT: This paper describes the strength-deformation and degradation aspects of ballast (latite basalt) tested in large-scale triaxial equipment under static and dynamic loading conditions. The influence of confining pressure and particle breakage on the ultimate shear strength, dilation rate and angle of internal friction is studied in detail. The effects of type of loading and number of load cycles on the settlement and degradation behaviour of ballast are discussed.

RÉSUMÉ: Ce document décrit les aspects de dégradation et de déformation dûe à la force du ballast (basalte latitique) testé daus une cellule triaxiale à grande échelle dans des conditions de chargement statiques et dynamiques. L'influence de la pression limité et de la rupture des particules sur la force de cisaillement ultime, le taux de dilatation et l'angle de friction interne est étudiée en détail. Les effets du type de chargement et du nombre de cycles de chargement sur le comportement de tassement et de dégradation du ballast sont examinés.

1 INTRODUCTION

Ballast degradation and track deformation is clearly associated with increased train frequency and heavier traffic loads, leading to significantly higher maintenance costs. For example, in New South Wales (NSW), approximately 1.3 million tonnes of ballast was consumed at a cost of over 12 million dollars during the 1992-93 period (Indraratna and Ionescu, 1999). In order to minimise maintenance costs, a thorough understanding of the strength-deformation-degradation behaviour of ballast under static and dynamic loading is essential.

Due to the relatively large size of ballast, conventional laboratory tests often give misleading stress-strain results and failure loads (Indraratna et al., 1998). To overcome the size effects, it is imperative to characterise these coarse aggregates by conducting tests using proportionately larger geotechnical equipment. With this in view, 'large-scale' triaxial facilities for testing ballast and rockfill materials have been designed and built in-house at the University of Wollongong. This paper elucidates the results of a major research program conducted in collaboration with the Rail Services Australia (RSA) of NSW, where static and dynamic testing of ballast (latite basalt) have been conducted.

The static and dynamic strength-deformation characteristics of ballast were studied using large-scale cylindrical and cubical triaxial rigs. In railway tracks, lateral displacement of ballast is not fully restrained. In order to simulate this field condition, the cubical triaxial rig was designed to facilitate lateral movement, instead of conventional rigid sides. Small lateral loads were applied to the movable sides to simulate the frictional resistance between the ballast and the track components, thereby representing the correct boundary conditions. The role of the magnitude of applied load and the number of load cycles on the deformation and degradation of ballast were the main factors of simulating the appropriate dynamic testing.

2 STATIC TRIAXIAL TESTING

Two different grades of latite ballast were used in the current study (Fig. 1). Gradations A and B are parallel to the upper limit and the lower limit of the 1983 State Rail Authority (SRA) specifications. The size of particles used in this study ranges between 10mm and 55mm. The sample size ratio, as defined by the diameter of the triaxial specimen divided by the maximum particle dimension, was about 5.7. It has been demonstrated that as the sample size ratio approaches 6, the size effects become negligible (Marachi et al., 1972; Indraratna et al. 1993).

An automated large-scale triaxial apparatus capable of accommodating specimens of 300 mm diameter x 600 mm high, was used for testing the ballast. The volume change of the specimen was determined by the movement of a coaxial piston located within a small cylindrical chamber (connected to the main cell), in which the smooth piston moves upwards or downwards depending on volume increase or decrease (Indraratna et al., 1998). The specimen was prepared inside a rubber membrane placed within a split cylindrical mould and compacted to represent typical bulk unit weights in the field (15.5 - 15.6 kN/m^3). The relative densities for gradation A varied from 46 - 61%, and from 52 - 63% for gradation B. Fully drained compression tests were conducted at relatively low confining pressures (10-300 kPa). The stress-strain behaviour was monitored up to about 20% axial strain, which included post-peak behaviour. In this study, the term 'failure' is defined by the state of maximum deviator stress, where mode of failure is considered to be 'bulging'.

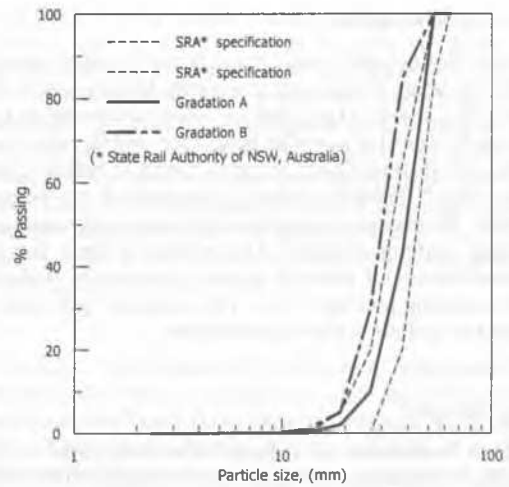

Fig. 1. Grain size distribution of railway ballast

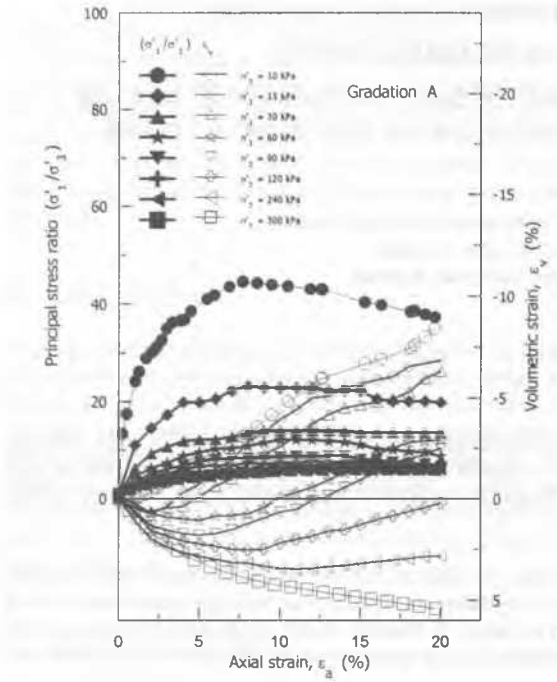

Fig. 2. Principal stress ratio and volumetric strain at various confining pressures (modified after Indraratna et al. 1998 with additional data)

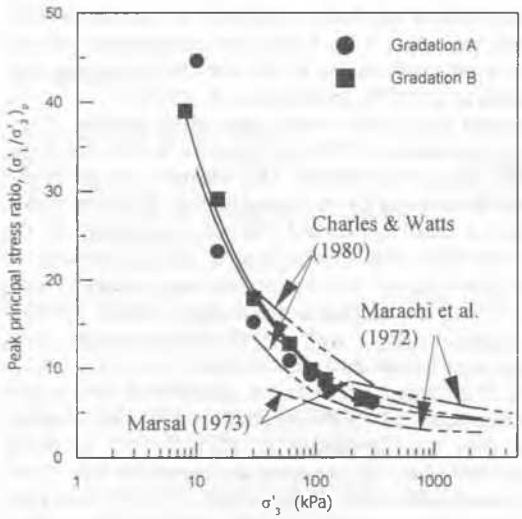

Fig. 3. Effect of confining pressure on peak stress ratio (modified after Indraratna et al. 1993, 1998)

2.1 *Stress-strain behaviour*

The results of isotropically consolidated drained triaxial tests for gradation A, in terms of principal stress ratio (σ'_1/σ'_3) and volumetric strain (ε_v) against axial strain (ε_a) plots, are shown in Fig. 2. Gradation B indicated a similar behaviour and therefore, not shown here. No distinct failure plane occurred in ballast specimens, even after 20% axial straining (post-peak). It can be seen in Fig. 2 that the maximum principal stress ratio decreases with the increasing confining pressure. The volumetric strain changes from dilation behaviour towards overall compression with the increasing confining pressure (σ'_3). The post-peak behaviour is characterised by a strain-softening behaviour.

2.2 *Shear strength*

The results of triaxial tests on railway ballast are plotted in Fig. 3, indicating the variation of the maximum principal stress ratio $(\sigma'_1/\sigma'_3)_p$ against the confining pressure. Selected rockfill data are also plotted for comparison. Although the current tests were

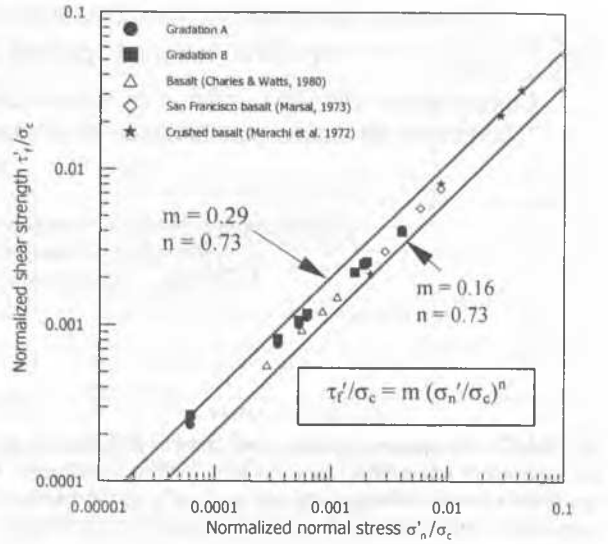

Fig. 4. Normalized stress-strength relationship for various aggregates (modified after Indraratna et al. 1993, 1998)

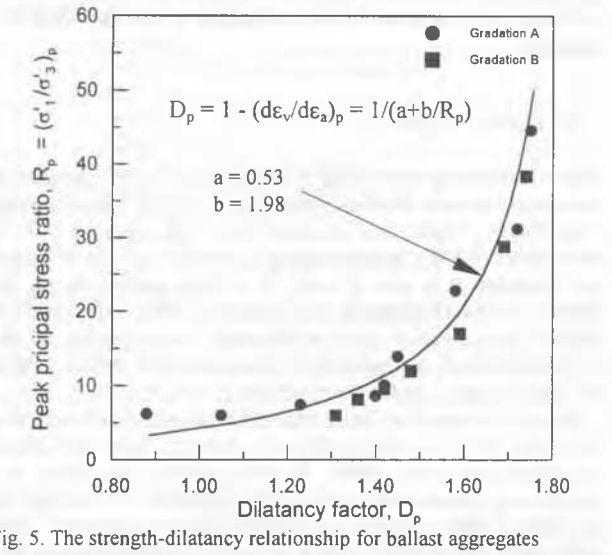

Fig. 5. The strength-dilatancy relationship for ballast aggregates

carried out at relatively low confining pressures, the results show a decreasing trend of $(\sigma'_1/\sigma'_3)_p$ with increasing σ'_3. Similar findings were also reported by other investigators (Marsal, 1973; Marachi et al., 1972; and Charles and Watts, 1980). As expected, gradation B having a denser packing of particles shows a slightly higher $(\sigma'_1/\sigma'_3)_p$ in comparison with gradation A. It is to be noted that while rockfill testing has usually been carried out at high confining pressures, railway ballast needs to be tested at relatively low confining pressure (10-200 kPa).

The shear strength of ballast is a function of the strength of parent rock and the level of confining pressure generated on track. Indraratna et al. (1993) proposed a dimensionless, non-linear strength criterion for rockfill, which can be extended to describe the behaviour of ballast at low confining pressure. This non-linear shear strength envelope is described by:

$$\tau_f/\sigma_c = m\,(\sigma_n/\sigma_c)^n \quad (1)$$

where, τ_f is the shear strength, σ_c is the uniaxial compressive strength of parent rock, σ_n is the normal stress, and m and n are dimensionless constants. The test data for latite basalt in a normalised form are plotted in Fig. 4, in comparison with other sources of basalt. Irrespective of the compressive strength, particle sizes and gradations of different types of basalt, all test results fall within a narrow margin, as shown in Fig. 4. For rela-

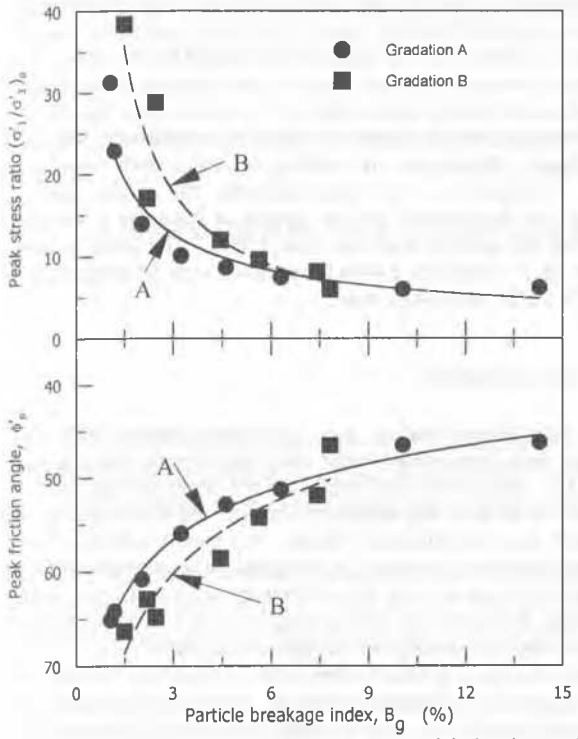

Fig. 6. Peak stress ratio, friction angle and particle breakage relation (modified after Indraratna et al. 1998)

tively small confining pressures (below 200 kPa), n takes values in the order of 0.70 - 0.75.

The effect of dilatancy on the maximum principal stress ratio $(\sigma'_1/\sigma'_3)_p$ is illustrated in Fig. 5, where dilatancy factor (D_p), is defined by $[1-(d\varepsilon_v/d\varepsilon_a)_p]$. Figure 5 shows that the relationship between $(\sigma'_1/\sigma'_3)_p$ and D_p is highly non-linear for the applied range of confining pressures. It has been argued that the rate of volume change at peak deviator stress decreases with increasing confining pressure, and that larger dilation rates $(-d\varepsilon_v/d\varepsilon_a)_p$ are associated with higher maximum principal stress ratio at low confining pressures (Charles and Watts, 1980).

2.3 *Particle degradation under static loading*

The degradation of particles under static triaxial loading was quantified by sieving ballast specimens (before and after each test) and recording the changes in the particle size distribution. Usually, small changes in particle sizes cannot be clearly illustrated in the conventional gradation plots. Therefore, an alternative method was developed by Marsal (1973), where the difference between the percentage retained by weight of each grain size fraction before and after the test (ΔW_k) was plotted against the aperture of the lower sieve corresponding to that fraction. In this technique, the particle breakage index (B_g), is equal to the sum of the positive values of ΔW_k, expressed as a percentage. Figure 6 illustrates the relationship between the particle breakage index with the maximum principal stress ratio and peak friction angle. It is clear from Fig. 6 that the reduction of $(\sigma'_1/\sigma'_3)_p$ and ϕ'_p is associated with increasing particle breakage. As expected, a higher degree of breakage was observed for gradation B, due to its greater initial density.

3 BALLAST BEHAVIOUR UNDER DYNAMIC LOADING

The deformation and degradation of ballast under dynamic triaxial loading was studied using a large-scale cubical triaxial equipment (Fig. 7). The cubical apparatus with movable sides can accommodate large specimens of size 800x600x600mm. The major principal stress (σ_1) is applied via a servo-hydraulic actuator through a 100mm steel ram, and the intermediate and minor

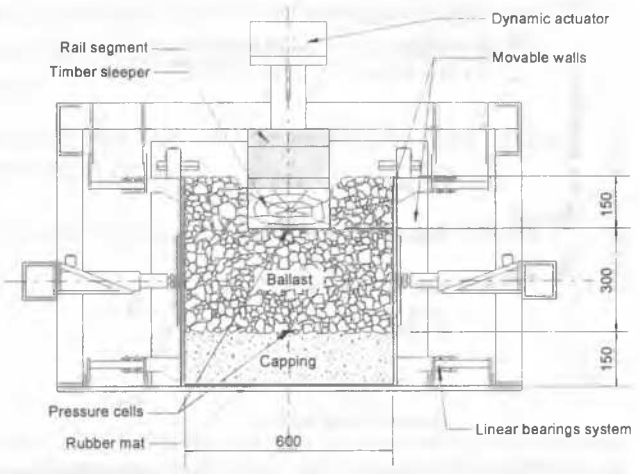

Fig. 7. Process simulation triaxial apparatus at University of Wollongong

principal stresses (σ_2 and σ_3) are applied using two pairs of hydraulic jacks with attached load cells. The minor principal stress (σ_3) models the effect of self-weight of ballast (shoulders and adjacent crib), and the intermediate principal stress (σ_2) models the transient stress between the sleepers and the self-weight of crib ballast. As no pore water pressures were considered for the free draining ballast, the total and effective stresses were assumed to be the same.

3.1 *Specimen preparation and test procedure*

The large triaxial box was filled with ballast in several layers, followed by the capping layer and a rubber mat at the bottom of the box to provide sufficient subgrade reaction (resilience). The compaction of capping and ballast layers was carried out to simulate field densities, using a vibrating compactor. Bulk unit weights of 16.7 kN/m^3 and 18.9 kN/m^3 were achieved for the ballast and capping layers, respectively.

The vertical load was applied to produce similar stresses caused by 25 tonne and 30 tonne axle loads in the track, which translate to 73 kN and 88 kN vertical load on the timber sleeper segment in the laboratory triaxial box. The tests were conducted at 15 Hz low-frequency level, maintaining a minimum seating load of 10 kN. The total number of cycles (one million) was selected to be compatible with 60 MGT of typical traffic loading.

3.2 *Ballast settlement under dynamic load*

Settlement of ballast under dynamic loading (up to 10^6 cycles) for different axle loads is shown in Fig. 8. Under dynamic loading, the initial settlement is rapid during the first 10,000-20,000 cycles. This is clearly due to the dynamic compaction of aggregates (stabilisation phase), which also takes place on new tracks or on recently maintained track. The rapid initial settlement is followed by gradual consolidation with increasing number of load cycles. It is also noted from Fig. 8 that as the load is increased from 25 to 30 tonnes axle load, a rapid settlement of ballast occurs. The subsequent settlements converge towards the ultimate settlement of the 30 tonnes/axle curve. The settlement of ballast under dynamic load is best modelled as a power-function of the number of load cycles:

$$S_N = a\, N^b \qquad (2)$$

where, S_N = settlement after N number of load cycles; N = number of load cycles; a = settlement after one load cycle; and b = empirical coefficient (non-linear regression). In the above equation, it is important to note that the variation of test parameters such as the magnitude of applied load and degree of compaction only affects the coefficient a, whereas b remains relatively unchanged.

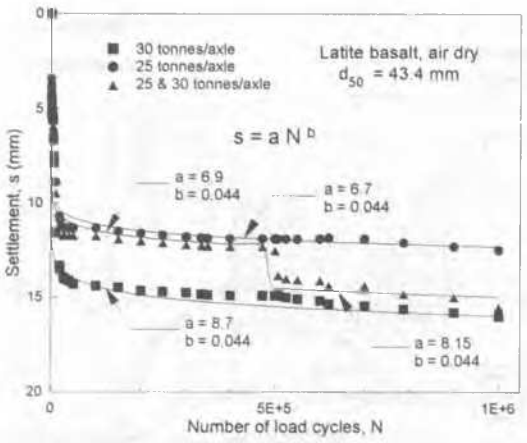

Fig. 8. Effect of load cycles and axle loads on settlement (after Indraratna and Ionescu, 1999)

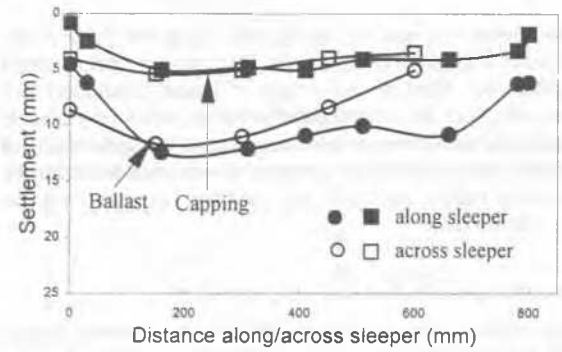

Fig. 9. Settlement of ballast and capping layer in dynamic testing (modified after Indraratna and Ionescu, 1999)

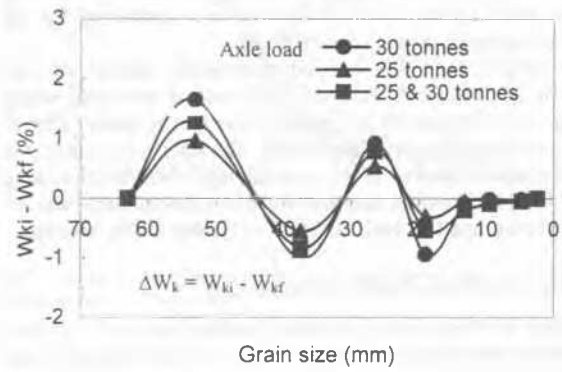

Fig. 10. Grain breakage in dynamic triaxial testing (modified after Indraratna and Ionescu, 1999)

In order to evaluate the contribution of individual layers of the laboratory model to the total settlement of the sleeper, the top level of the aggregate layers (i.e. ballast and capping layers) was measured at the end of each test. On the basis of laboratory measurements, it was found that more than 60% of the total settlement was attributed to the deformation of ballast layer caused by 88 kN cyclic loading (Fig. 9).

3.3 *Ballast degradation in dynamic testing*

In order to evaluate the degradation characteristics of latite ballast under dynamic loading, the difference in percentage of particle weight retained in each sieve before and after testing, ΔW_k was measured and plotted against lower sieve size (Fig. 10). The positive values of ΔW_k in Fig. 10 indicate the degradation of the corresponding particle size more than the total accumulated crushed particles from the higher grain sizes, and conversely, the negative values of ΔW_k indicate the degradation of the corresponding particle size less than the accumulated crushed particles from the higher grain sizes. It is evident from Fig. 10 that the breakage mainly affects the larger size particles in the order of 55mm. The degree of crushing increases with the applied load. Irrespective of the load amplitude, the smaller particles suffer less degradation, and the degree of breakage is insignificant for the particle sizes less than 15mm. The grain breakage index (B_g) varies from 2.44% for tests run with 30 tonnes/axle to 1.51% for 25 tonnes/axle load.

4 CONCLUSIONS

The strength-deformation and degradation aspects of railway ballast were investigated under static and dynamic triaxial loading. The test results confirmed that the shear strength and the degree of particle degradation (breakage) are influenced by the particle size distribution of ballast, but mostly affected by the applied confining pressure. A modified shear strength criterion (non-linear) can be used for preliminary design of track. In this criterion, the shear and normal stresses at failure are normalised by the uniaxial compressive strength of the parent rock.

The maximum principal stress ratio is found to decrease with the increasing confining pressure, where pronounced non-linearity is evident at small confining pressures. The higher principal stress ratio at low confining pressure is associated with lower degree of particle breakage, which in turn, contributes to increased rate of dilation. Laboratory data have shown that the maximum principal stress ratio and peak friction angle are reduced by increasing particle degradation (breakage) at higher confining pressures. At elevated confining pressures where dilation is suppressed, the breakage index, B_g increases substantially.

Dynamic, cubical triaxial tests provide a more comprehensive picture of load-settlement and particle degradation behaviour, because the speed and frequency of trains impart a quasi-cyclic load on the ballasted foundation, generating non-uniform vibrations. The test results clearly illustrate that the ballast aggregates stabilise rapidly during the first 10,000 -20,000 loading cycles after the newly constructed track or maintenance cycle. The rapid initial settlement is followed by gradual consolidation with increasing loading cycles. An increase in axle load causes an additional period of rapid settlement. It is concluded from dynamic triaxial tests that particle sizes of 50-55mm undergo considerable degradation, while the smaller particles less than 15mm experience insignificant breakage.

REFERENCES

Charles, J. A. and Watts, K. S. (1980). The influence of confining pressure on the shear strength of compacted rockfill, *Geotechnique*, 30(4), 353-367.

Indraratna, B., Ionescu, D. and Christie, H. D. (1998). Shear behavior of railway ballast based on large scale triaxial tests, *ASCE Jnl. of Geotechnical and Geoenvironmental Engg.* 124(5), 439-449.

Indraratna, B., Wijewardena, L. S. S. and Balasubramaniam, A. S. (1993). Large-scale triaxial testing of greywacke rockfill. *Geotechnique*, Vol. 43, No. 1, pp. 37-51.

Indraratna, B. and Ionescu, D. (1999). Deformation of ballast under static and dynamic loading, *Prefailure and deformaton characteristics of geomaterials.*, Jamiolkowski et al. (eds), 283-290.

Marachi, N.D., Chan, C.K. and Seed, H.B. (1972). Evaluation of properties of rockfill materials, *J. Soil Mech. and Found. Engg.*, A.S.C.E., Vol. 98, 95-114.

Marsal, R.J. (1973). Mechanical properties of rockfill, *Embankment Dam Engineering, Casagrande Volume*, Wiley, pp. 109-200.